Department of Radiology and Nuclear Medicine,
Amsterdam University Medical Centre, Amsterdam AMC
(Head: Prof. PhD Jaap Stoker)

Acute Stress Effects on Prefrontal Cortex GABA and Glutamate Concentrations, and their Correlations to Electrocardiographic Markers

Bachelor Thesis

University of Veterinary Medicine Vienna

Submitted by

Tin Jurhar

Amsterdam, June 2020

Supervised by:

Dipl.-Biol. Dr.rer.nat. Rudolf Moldzio

Ass.Prof. Anouk Schrantee, PhD

Antonia Kaiser, MSc

Reviewed by:

Univ.-Prof. Dr.med. Elena Pohl

Acknowledgement

What is stress? When I started this project, I asked myself how I could know so little about something I thought I knew so well. The past nine months have not only provided me with tremendous insight into new fields of research and methodology, they have also taught me the importance of challenging my own intuition in the process. Credit where credit is due, this experience would not have been the same without the people who supported me throughout it.

First of all, I want to express my deepest gratitude to my internship supervisors Anouk Schrantee and Antonia Kaiser. Thank you, Anouk, for accepting me into the BrainBeatS project in the first place, for encouraging me to take on the challenges this extensive internship would bring, and for always sparing an extra minute to answer a question at times you were already running late. Antonia, thank you in particular for your expertise and guidance on a daily basis. You have been incredibly patient in your explanations and trusting in my work from the very beginning. Your wit has made countless scan nights all the more enjoyable.

I also wish to thank Liesbeth Reneman for having me participate in her project and Aart Nederveen on behalf of the z0 staff and students for creating a welcoming and inclusive work environment. Sean, I appreciate all the exchange of silly and serious notions, and Joy, you were an incredible addition to the scanning team.

Special thanks to my internal supervisor Rudolf Moldzio for his flexibility and phone call consultations, for his helpful insights throughout my internship, and for making the experience of writing my thesis abroad unbelievably easy. I also wish to thank Marlies Dolezal from the University of Veterinary Medicine Vienna's biostatistics platform for her engagement in data analysis towards the end.

Lastly, all this would not have been possible without my family and friends; mom, Pia, Jesse, thank you for the visits, care packages, all the video calls and relentless support.

Table of Contents

1. The Human Stress System

The human stress response is defined as a systemic effort to maintain homeostatic balance under real, perceived, or anticipated threat (McEwen, 2000). Dependent on the type of stressor (e.g. psychogenic, physical, chemical) this response can either be behavioral or take the form of adjustments to the internal milieu, a dynamic process summarized under the concept of allostasis (Sterling & Eyer, 1988). The result is the body's adaptation to changing energetic demands through long- and short-term regulatory networks.

A dysregulation in the stress system through prolonged or over-intensive activation has been linked to a multitude of mental and physical conditions. Stressful life events underlie post-traumatic stress disorders, promote drug seeking behavior (Shaham & Stewart, 1995; Sharp, 2017), onset of major depressive episodes (Kendler, Karkowski, & Prescott, 1999), and increase risk of psychosis (Day et al., 1987; Varese et al., 2012). There is evidence suggesting stress increases susceptibility to viral infections of the upper respiratory tract (Cohen, Tyrrell, & Smith, 1991; Murphy et al., 2008) and facilitates progression of inflammation (Cole et al., 2007), atherosclerosis and coronary heart disease (Steptoe & Kivimäki, 2012). Further, severe mental stress can acutely worsen myocardial ischemia (Goldberg et al., 1996; Gottdiener et al., 1994) and induce cardiomyopathies in otherwise healthy individuals that are clinically indistinguishable from cardiac infarction (Prasad, Lerman, & Rihal, 2008; Sinning et al, 2010; Tamplin et al, 2015). The severity of these consequences makes stress not only a target of holistic treatments, but also of emergency medicine. A new importance is placed on understanding the underlying mechanisms of the stress response, particularly in the context of cardiac regulation.

The far-reaching effects of stress system (dys-)function already suggest its integration into several physiological systems. It is comprised of a central nervous regulatory component and its autonomic and neuroendocrine effector branches (Chrousos & Gold, 1992). The two effector branches distribute stress signals to target tissues and elicit change in energy distribution and metabolic activity either through direct innervation (e.g. of the heart) or through mediators such

as cortisol, catecholamines, and cytokines. These end products also provide feedback to the central nervous system (CNS), which assesses appropriate duration and intensity of the response.

1.1 The Autonomic Stress Response

The autonomic stress system constitutes the body's immediate response to stress. It is comprised of sympathetic and parasympathetic fibers and the adrenal medulla, whose stimulation triggers synthesis and release of catecholamines epinephrine and norepinephrine into the bloodstream (Ulrich-Lai & Herman, 2009). While the sympathetic branch is understood to be initiator of the stress response, the parasympathetic branch is seen as a regulator of autonomic activity.

The sympathetic division of the autonomic stress system receives its input from cholinergic neurons in the intermediolateral cell column and the central autonomic area of the spinal cord. These project through spinal segments T1 (thoracic) to L3 (lumbar) and relay in the three medially located prevertebral ganglia and the bilaterally organized sympathetic trunk. From there, efferent fibers innervate target tissue, including the adrenal medulla, the heart, blood vessels, bronchial airways, piloerector muscles, and salivary and sweat glands, as well as the organs of the gastrointestinal tract (Purves, 2018). Parasympathetic ganglia are located close to or within their effector organs, and receive CNS input from cranial nerves III (*N. oculomotorius*), VII (*N. facialis*), IX (*N. glossopharyngeus*), and X (*N. vagus*), as well as from efferents of the sacral spinal segments S2-S4.

Sympathetic arousal and subsequent catecholamine release from chromaffin cells of the adrenal medulla signifies the initiation of the autonomic, so-called sympatho-adrenomedullary (SAM), response. This occurs either via top-down control from cortical structures or reflexively through peripheral signals of homeostatic perturbation, such as blood loss, respiratory distress, pain, and inflammation (Ulrich-Lai & Herman, 2009). Circulating epinephrine and norepinephrine then interact with adrenergic receptors in different tissues to modulate metabolic and cardiovascular behavior (for a detailed review, see Tank & Wong, 2015). Taken together, the SAM prepares the body for *fight-or-flight* by effecting an increase in heart rate, blood pressure, and

respiration, through energy mobilization in fat and liver tissue, and through redirecting blood supply from the viscera to skeletal muscle.

The parasympathetic division plays a lesser role in stress initiation and is more involved in mediating the duration of the autonomic response. It generally counteracts SAM effects and is activated upon sympathetic arousal over reflex arcs or through interaction of circulating catecholamines with vagal adrenoreceptors (Tank & Wong, 2015). This feedback is largely gated through the nucleus of the solitary tract (NTS) in the brainstem, a large hub for viscero- and somatosensory information (Purves, 2018). In addition, a part of the signal is forwarded by norepinephrine neurons in and around the NTS to higher-order thalamic and cortical structures, allowing for integration with neuroendocrine and behavioral responses.

1.2 Neuroendocrine Stress Response

Peripheral stress adaptations beyond the targets of the SAM are mediated by the hypothalamus-pituitary-adrenocortical axis (HPA) with glucocorticoid cortisol as the end product. The peripheral stress system is schematically depicted in *Figure 1*. HPA activity governs the body's energy household over longer time periods, naturally peaking in the morning just before waking and decreasing as the day progresses (Russell & Lightman, 2019). During stress, this circadian activation pattern is interrupted in favor of phasic cortisol release and subsequent tightening of metabolic tone.

Arousal of the HPA occurs almost exclusively via the paraventricular nucleus of the thalamus (PVN), through peripheral signals from the brainstem, and through signals of the cortex. These signals are then forwarded to the anterior pituitary through release of, amongst others, the neurohormones corticotropin-releasing hormone and arginine vasopressin (Spencer, Robert L & Deak, 2017). The pituitary responds by increasing release of adrenocorticotropin into the systemic blood stream, a peptide that stimulates cortisol synthesis in cells of the adrenal cortex. Cortisol continues to have fast-acting metabolic and long-term genomic effects via signaling through membrane and nuclear receptors on target tissue, respectively. These include arrestation of certain immune functions (Segerstrom & Miller, 2004), hypertension through increase in blood volume, and induction of catabolic processes in the carbohydrate, protein and fat

metabolism (Russell & Lightman, 2019). Plasma cortisol peaks about 20 minutes after stress onset (Droste et al., 2008), whereas modulations on the genomic level take effect after several hours (Van Ast, Cornelisse, Meeter, Joëls, & Kindt, 2013). Attenuation occurs in a negative-feedback manner on the level of the pituitary, the PVN, and the hippocampus (Ulrich-Lai & Herman, 2009).

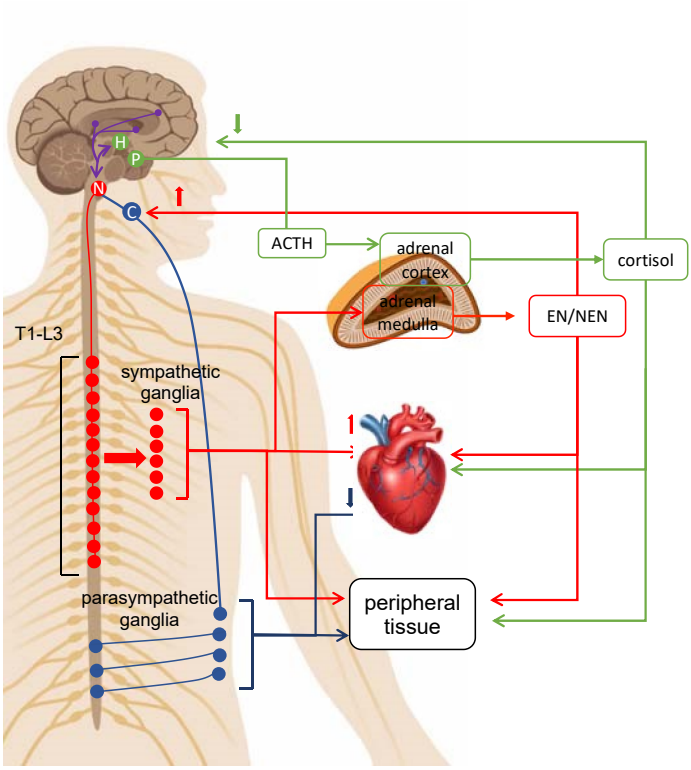

Figure 1 Overview of the Peripheral Stress System. *The peripheral stress system and its sympatho-adrenomedullary (red) and hypothalamus-pituitary-adrenocortical (green) axes. The SAM receives CNS input via brainstem structures such as the nucleus of the solitary tract (N) and acts either through direct innervation of target tissue (such as the heart) or intermediarily through the adrenal medulla, which releases catecholamines (EN/NEN) into the bloodstream. EN/NEN also serve as mediators to the SAM through interaction with vagal catecholamine receptors (C). The HPA is activated in the paraventricular nucleus of the hypothalamus (H), which in turn causes release of adrenocorticotropin (ACTH) in the pituitary (P). End product is cortisol. Stimulating/inhibitory effects are indicated with up/down arrows, respectively. CNS regulatory sites are shown in purple.*

1.3 The Central Nervous Stress System

Autonomic and neuroendocrine effector branches are not always activated in the same manner, rather stressors of different qualities elicit finely differentiated response patterns (Taggart,

Critchley, van Duijvendoden, & Lambiase, 2016; Tank & Wong, 2015). This requires an extensive amount of cross-integration of the two networks, a task that is taken on by a diffuse network within CNS. Together with adjusting and integrating peripheral responses, the CNS also reacts to psychogenic stressors and integrates these into emotional and cognitive processes (van Oort et al., 2017), ultimately assessing and coordinating adequate behavioral response (e.g. fight-or-flight). This section aims to give a brief overview of these CNS functions and their respective anatomical parts.

1.3.1 Regulation of Peripheral Stress Responses

Processing of peripheral stress signals occurs on several hierarchical levels. Autonomic feedback that reaches the CNS through the NTS directly activates the HPA via projections into the PVN (Cunningham, Bohn, & Sawchenko, 1990), establishing an immediate connection between the HPA and SAM. The NTS further targets reflex centers in the brainstem to allow immediate adjustments to vital regulatory circuits (Ulrich-Lai & Herman, 2009). Higher-order processing of autonomic signals is performed by the hypothalamus, amygdala, as well as the insular cortex and the dorsal anterior cingulate cortex (dACC) of the medial prefrontal cortex (mPFC). Though, the exact mechanisms of their involvement in peripheral stress regulation is yet to be understood (Sklerov, Dayan, & Browner, 2019). In general, activity in each of these regions influences the net output of sympathetic and parasympathetic arousal (Sklerov et al., 2019).

The CNS also responds to HPA signals through cortisol receptors. These can be found throughout the brain, yet HPA regulation is largely taken on by the basal ganglia and limbic structures such as the hippocampus and the medial amygdala (Herman et al., 2003). Upon detection of circulating cortisol (as a highly lipophilic molecule it is permitted through the blood-brain barrier), these structures suppress PVN activity through direct and indirect γ-aminobutyric acid (GABA) pathways, resulting in negative-feedback regulation of the endocrine response.

1.3.2 CNS Adaptations in Stress

Unlike in the periphery, there is no single mechanism that signifies the CNS stress response. Instead, the central nervous stress response is understood to be a shift in activity from default

operational networks to ones more likely to meet present challenges (Hermans, Henckens, Joëls, & Fernández, 2014). The characterization of these networks heavily relies on functional magnetic resonance imaging (fMRI) observation of experimentally induced stress states. Definitions might therefore vary dependent on the method of stress induction. Nonetheless, the past two decades of fMRI research identified three brain networks most involved in stress responses, the default mode network (DMN), the salience network (SN), and the central executive network (CEN) (Hermans et al., 2014).

The DMN comprises those brain regions most active during resting state, while no cognitive task is being performed. It centers around the dorsal mPFC, the precuneus and the posterior cingulate cortex which engage in self-referential processing and emotional regulation, in memory processing, and in consciousness, respectively (Andrews-Hanna, Reidler, Sepulcre, Poulin, & Buckner, 2010; Fransson & Marrelec, 2008). Activity of the DMN increases throughout most stress induction paradigms (e.g. viewing of distressing images, social stress tasks) (van Oort et al., 2017), but can at least in part be downregulated via higher-order cognitive processing (Koric et al., 2012).

The SN and CEN play a role at an early and later stage during the stress response, respectively. Accompanying enhanced connectivity within the DMN is an activation of the SN (Sinha, Lacadie, Skudlarski, & Wexler, 2004; van Marle, Hermans, Qin, & Fernández, 2010), which is proposed to induce a hypervigilant state to promote emotional sensitivity, chances of threat detection (van Marle, Hermans, Qin, & Fernández, 2009), and fast stimulus-oriented behavior (Corbetta, Patel, & Shulman, 2008). The prefronto-limbic dACC, anterior insula, temporal pole, and the amygdala are structures strongly associated with these tasks (van Oort et al., 2017).
SN activity eventually is downregulated and succeeded by the CEN. The CEN mediates higher-order cognitive functions of importance to problem solving at the late phase of the stress response, such as decision making, goal-oriented planning, working memory, and directing attention (Hermans et al., 2014). A detailed account of the SN and CEN, as well as their activation in relation to peripheral stress responses, is given in *Figure 2*.

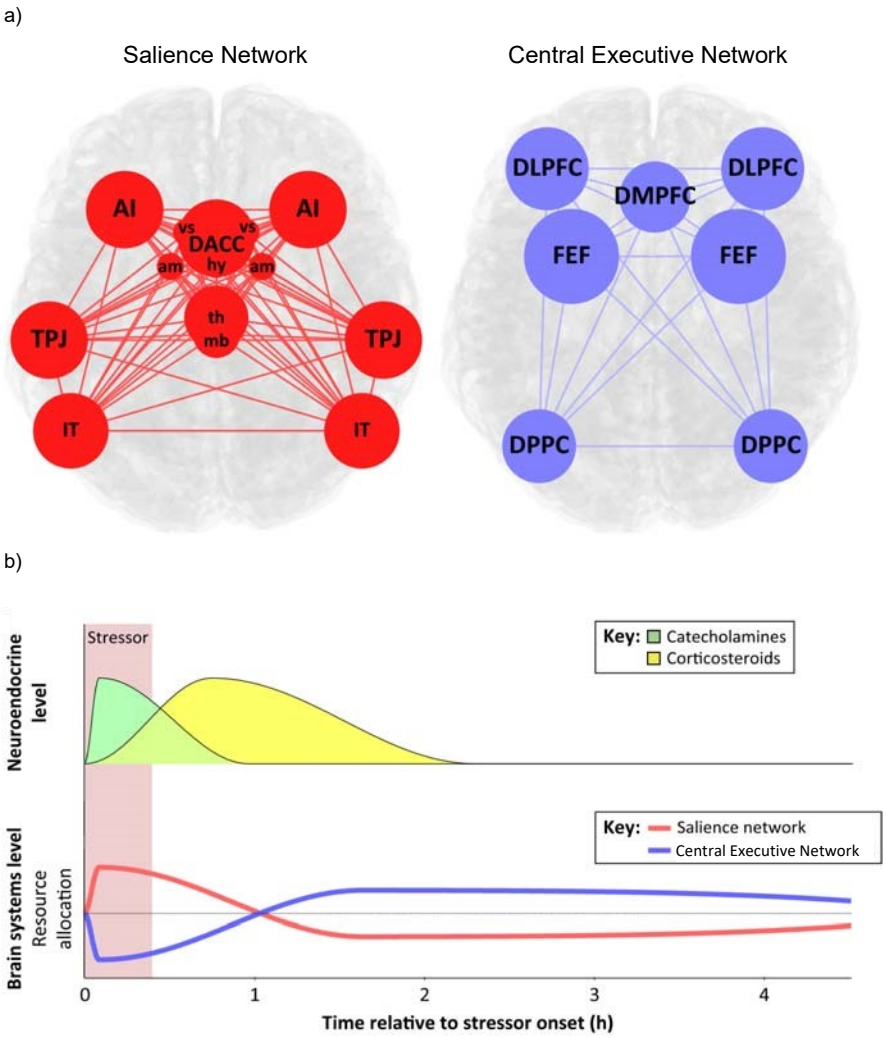

Figure 2 CNS Activity during Stress and Comparison to Peripheral Stress Responses. *(a) Activity in the salience (left) and central executive network (right) marks the central nervous stress response. Structures of the SN include the amygdala(am), the dorsal anterior cingulate cortex (DACC), anterior insula (AI), inferotemporal cortex (IT), midbrain (mb), thalamus (th), temperoparietal junction (TPJ), ventral striatum (vs). The CEN is associated with the dorsolateral prefrontal cortex (DLPFC), the dorsomedial prefrontal cortex (DMPFC), dorsal posterior parietal cortex (DPPC), and the frontal eye fields (FEF). (b) shows the role of peripheral (top) and central nervous (bottom) response systems at different times after stress onset. Sympathetic catecholaminergic pathways and the SN are immediate responders to stress, followed by cortisol- (corticosteroid) mediated effects. SN activity gradually is succeeded by the CEN.*

1.3.3 Regulation of CNS Response

With the mapping of cortical networks involved in the stress response, there is increasing interest in understanding what regulates their activity. On a systems level, the importance of GABAergic pathways in stress regulation is widely recognized. GABA-receptor antagonists such as bicuculline are categorized as anxiogenic, whereas GABA-receptor agonistic medication is commonly prescribed for their anxiolytic effects (Delli Pizzi et al., 2017). Further, withdrawal from GABA-receptor agonistic baclofen has shown to induce cardiomyopathies similar to those

induced by severe stress (Levy, De Brier, Hugeron, Lansaman, & Bensmail, 2016), suggesting GABAergic involvement in autonomic regulation.

Reactivity of the mPFC also depends on a small population of GABAergic interneurons (Courtin et al., 2014). The mPFC receives input from the sensory cortices and directly projects to the limbic system, as well as control sites of the SAM and HPA, exerting top-down control of emotional and peripheral stress responses (Ellard, Barlow, Whitfield-Gabrieli, Gabrieli, & Deckersbach, 2017). These pathways are largely mediated by glutamatergic neurons, the role of GABA as their primary regulator under stress is still subject to investigation. While one study was able to show prefrontal GABA concentrations decrease in immediate response to stress (Hasler, van der Veen, Grillon, Drevets, & Shen, 2010), another (Houtepen et al., 2017**)** did not replicate these findings. A third study investigated GABA in the dACC outside of the stress context and found GABA to be a reliable predictor of connectivity between the prefrontal cortex and limbic system (Delli Pizzi et al., 2017). These structures are strongly associated with the SN, again pointing towards involvement of GABA in CNS stress regulation.

2. Technical Background

Non-invasive *in-situ* determination of neurometabolite concentrations is currently only possible with the help of magnetic resonance spectroscopy (MRS). In MRS, ^{1}H-MRS specifically, hydrogen's changing magnetic resonance properties in different chemical environments are used to distinguish between constituents of a tissue. This section aims to provide a contextual overview of MRS methodology and its relevance in systems-level GABA research.

2.1 ^{1}H-MRS Principles

Generation of an MRS signal is based on two fundamental principles: (1) atomic nuclei intrinsically possess magnetic properties, and (2) a change in magnetic field induces an electrical current. When exposing a sample to a strong external magnetic field (B_0), the net magnetic field of nuclei (M) will tendentially align with it. In ^{1}H-MRS, hydrogen atoms are selectively excited with an electromagnetic radiofrequency (RF) pulse which causes a reorientation of M into the transverse plane of B_0 (de Graaf, 2019). Within a few milliseconds the excitation subsides and M will oscillate back into alignment with B_0. This change in M induces an electrical current in a nearby receive coil, which is recorded as the metabolite signal. *Figure 3* illustrates this process. In practice, the amount and quality of RF pulses vary depending on the pulse sequence and research design (Bertholdo, Watcharakorn, & Castillo, 2013), however, these will not be discussed within this section.

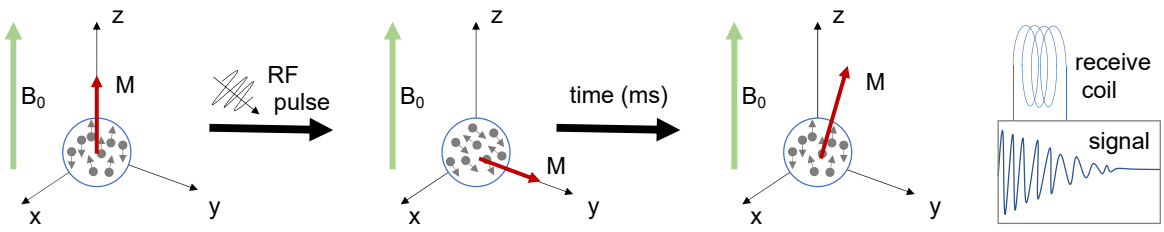

Figure 3 Principle of ^{1}H-MRS Signal Generation. *The net magnetic field of atomic nuclei within a sample (M) aligns with the magnetic field of the MRS scanner (B_0). ^{1}H atoms are then selectively excited with a radiofrequency (RF) electromagnetic pulse which reorients M into the transverse plane of B_0. As M oscillates back into alignment with B_0, it induces a signal current in a nearby receive coil.*

2.1.1 Signal differentiation in ^{1}H-MRS

The oscillation frequency (also referred to as resonance frequency) at which M precesses around B_0 depends on several factors: the field strength of B_0, the spin properties of ^{1}H, as well

as the chemical environment in which the nuclei reside (de Graaf, 2019). The latter is of high relevance to MRS as it implies hydrogen atoms of different chemical compounds produce signals deviating from the standard resonance frequency of ^{1}H. These deviations in frequency, or chemical shifts, lie within the range of 10^{-6} (parts per million, ppm) and are used to determine individual contributors to the overall signal, such as GABA and glutamate. After application of a Fourier transform, signals of distinct ^{1}H groups are represented on a frequency spectrum by peaks (see Methods, *Figure 6d*). The area under the curve of each peak is approximately proportional to its concentration in the tissue.

2.1.1 Spatial Encoding

Clinical MRS is most commonly applied to a small volume (voxel) of several millimeters within the brain, although methods for multi-voxel spectroscopic imaging do exist (Bertholdo et al., 2013). In order to distinguish between signals from a voxel of interest and its surrounding tissue, spatial encoding techniques have to be applied. Spatial encoding entails application of orthogonal RF pulses that selectively excite in the x,y, and z plane; the voxel is defined by the intersection of those planes (Bottomley, 1987). These pulses are coupled with intentional heterogenizations of the external magnetic field such that the resonance frequencies for ^{1}H within the region of interest contrast those in the remaining tissue.

2.1.2 Water and Lipid Suppression

Lipid and water suppression have to be performed prior to application of a pulse sequence, as signal from these compounds influence the accuracy and resolution of metabolite signal recording. Water concentration in neural tissue exceeds that of metabolites by a 10,000-fold (de Graaf, 2019). In order to minimize its contribution to the overall signal, frequency-selective pulses (Mescher, Merkle, Kirsch, Garwood, & Gruetter, 1998) at the resonance frequency of water at approximately 4.7 ppm are applied. Lipid signal, on the other hand, stems from adipose tissue surrounding the brain, and can be reduced with the help of spatial-selective excitation pulses (Felmlee & Ehman, 1987).

2.2 Biological Implications of GABA MRS Research

Recent methodological improvements, such as advancement to ultra-high field MRS (≥ 7 Tesla) have allowed for more precise neurometabolites recordings (Terpstra et al., 2016). These developments open up new possibilities of investigating neurotransmitters found in increasingly lower concentrations in the brain such as GABA. However, there are limitations in the insight these data give into the biochemical functioning of GABA-mediated neuronal inhibition.

GABA and other neurotransmitters involved in synaptic signaling are understood to be presynthesized and stored intravesicularly within neurons until a rise in cell membrane potential facilitates their release into the synaptic cleft. Signal transduction is thus not dependent on the net concentration of a neurotransmitter, but rather on its relative intra- and extracellular distribution. Nonetheless, with MRS, changes in GABA concentration across voxels of several millimeters can be detected in immediate response to different experimental tasks (Chen et al., 2017; Cuypers et al., 2020; Hasler et al., 2010).
This apparent confliction has previously been addressed in literature (Stagg, Bachtiar, & Johansen-Berg, 2011), but there is no consensus on which biochemical processes govern region-wide changes in GABA concentration. While evidence exists for the involvement of glial cells in the extra-neuronal regulation of GABA (Preece & Cerdán, 2002; Yoon et al., 2011), more recent findings estimate the effect of these mechanisms to be relatively low (Lee et al., 2010; Santhakumar, 2006). Moreover, it has not been shown whether MRS differentiates between intravesicular and extravesicular, intracellular and extracellular, or intrasynaptic and extrasynaptic GABA.

The mechanisms behind region-wide increases of GABA thus remain to be understood, yet functional correlations between GABA concentration and brain region activity have been established. While these grant further investigation of GABA involvement in higher-order processing, they give no insight into the underlying mechanisms on the (sub-)cellular level.

3. Research Aims

The importance of prefronto-limbic structures such as the dACC and GABA pathways in stress regulation is widely recognized. However, how and where these systems interact is still subject to research. In consideration of recent efforts to understand the regulation of prefrontal activity (Delli Pizzi et al., 2017; Hasler et al., 2010; Houtepen et al., 2017), this study aims to further investigate GABA and glutamate behavior in the dACC in response to acute stress. In the case we observe a link between stress prefrontal GABA concentrations, we consider the dACC a candidate integrator of GABAergic signals into the central nervous and autonomic cardiac stress response. Specifically, we expect prefrontal GABA concentrations to be lower in stressed individuals than in controls, as well as to record higher HPA and SAM output. We wish to contextualize spectroscopic data with measures of cardiac and cortisol response, explore the possibility of temporal dependencies between the three and assess possible predictors of stress vulnerability.

4. Methods

This study was conducted at the Spinoza Centre for Neuroimaging in Amsterdam, Netherlands and is in accordance with the Declaration of Helsinki (1997) and subsequent revisions, its experimental protocol was approved by the ethics board of the University of Amsterdam.

4.1 Participants

We included 56 psychologically and physically healthy males (mean = 24.18 years, SD = 2.82). They were recruited through posters and digital advertisements within the greater Amsterdam area. Inclusion criteria were 1) age between 18 and 35, 2) no diagnosis of a psychiatric, neurologic, or cardiovascular condition, and 3) Dutch and English proficiency. Exclusion criteria were 1) smoking, 2) any cardiac abnormality as determined by an electrocardiogram (ECG), 3) excessive alcohol and drug intake, assessed with the Alcohol Use Disorders Identification Test (AUDIT, score > 11)(Saunders et al., 1993) and the Drug Use Disorders Identification Test (DUDIT, score > 11) (Berman, Bergman, Palmstierna, & Schlyter, 2003), respectively, 4) MRI contra-indications, and 5) high self-reported stress levels as determined on the Perceived Stress Scale (PSS, score > 26) (Cohen, Kamarck, & Mermelstein, 1983). The experiment was set up as a between-subject study with an equally large stress and control group matched on age, AUDIT, DUDIT, and PSS scores, as well as on IQ reflected by performance on the Dutch Adult Reading Test (Mulder & Bouma, 2012).

4.2 Questionnaires

Additional questionnaires acquired were the Beck Depression Inventory II (Beck, Steer, & Brown, 1996), the Symptom Checklist-90 Revised SCL-90-R (Pearson, United States), the Trait Scale of the State-Trait Anxiety Inventory STAI-T (Marteau & Bekker, 1992), the Life Event Questionnaire (Garnefski & Kraaij, 2001) for investigation of longer-term and past stress-related life episodes, as well as a brief form of the Positive and Negative Affect Schedule PANAS-SF (Watson, Clark, & Tellegen, 1988), which reflects current emotional state.

4.3 Experimental Procedure

Participants were invited to the facility twice, once for a pre-examination and once for the scanning appointment. The pre-examination included a ten-lead ECG, completion of questionnaires, and retrieval of written informed consent. Scanning appointments were scheduled between 14:30 and 21:00 h to account for circadian cycling of blood cortisol. Participants were instructed to refrain from exercise, caffeine-, drug-, and alcohol consumption for up to 24 hours prior, and not to eat in the three hours leading up to their appointment. Upon arrival they were given 45 minutes of acclimatization time, during which a 10-second-long baseline ECG was recorded. The scan session itself lasted approximately ninety minutes and consisted of a pre-intervention MRS and function magnetic resonance imaging (fMRI) scan (25minutes), a stress or control intervention (15 minutes), and two respective post-intervention measurements (50 minutes). Upon completion, we recorded another one-minute-long post-intervention ECG.

Salivary cortisol content of participants was sampled at five timepoints during the experimental procedure as a measure of HPA response. These timepoints can be extracted from the schematic procedural overview in *Figure 4.* Saliva samples were collected with a cotton swab and stored in Salivette© (SARSTEDT AG & Co. KG, Nümbrecht, Germany) cortisol tubes (batch number 51/05) at - 20 ºC until analysis.

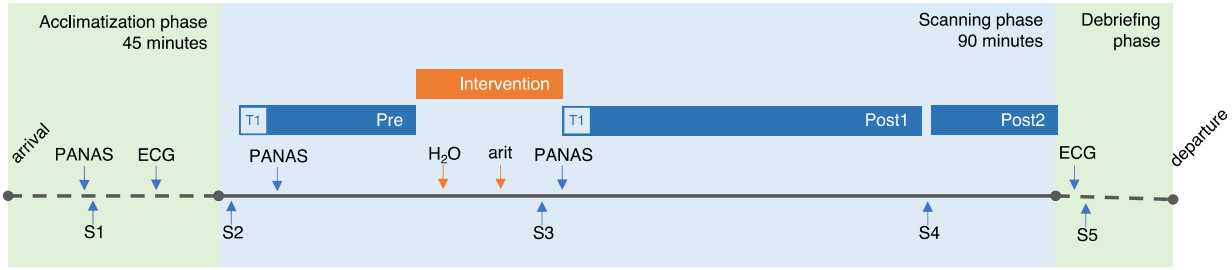

Figure 4 Schematic Overview of Scan Appointment. *Scan appointment lasted about 2.5 hours in total and can be divided into three phases: acclimatization, scanning, and debriefing. Upon arrival of the participant, a baseline ECG and emotional report (PANAS) were acquired. Timepoints of saliva sampling for monitoring of cortisol response are denoted with S1-5. MRS scanning consisted of one pre-intervention (Pre) and two post-intervention (Post1, Post2) scans, a T1-weighted image provided an anatomical overview for voxel selection. The beginning of the water (H_2O) and arithmetic (arit) task of the intervention are marked in orange. Two additional PANAS and one ECG were recorded at the indicated timepoints.*

4.4 Intervention: Socially Evaluated Cold Pressor Task

The stress task performed was an adapted Socially Evaluated Cold Pressure Task (SECPT) (Schwabe, Haddad, & Schächinger, 2008), which combines psychological (social evaluation)

and physical (cold water) stressors into one paradigm. All trials were executed by the same male experimenter whom none of the participants beforehand knew. In the stress condition, the experimenter was wearing a white coat and gloves and maintained a neutral expression. After short instructions the participant's right foot was submerged into a bucket of cold water (0 – 4 ºC) for three minutes, followed by a three-minute arithmetic subtraction task. In the control condition, the experimenter wore street clothing and was encouraged to give friendly, positive feedback. The cold water was replaced by warm water (20 – 22 ºC) and the participants were given simple additions to solve instead of subtractions.

4.5 Defining Cardiac Parameters

Electrocardiograms were recorded on a 10-lead ECG system and evaluated by an in-house condition-blind cardiologist in terms of significant changes between pre- and post-intervention measurements. Additionally, heart rate of participants during scans and stress intervention was recorded with a scanner-integrated plethysmographic pulse oximeter, as it is widely recognized to be a reliable indicator of sympathetic response. Heart rate measurements were imported to, and corrected for outliers in MatLab (R2016a, Version 9.0.0.341360) using in-house developed scripts.

4.6 ^{1}H Magnetic Resonance Spectroscopy

4.6.1 MRS Data Acquisition

All data was acquired using a Philips 7T Achieva MR scanner (Philips Medical Systems, The Netherlands) equipped with a 32 channel-phased array head receive coil. ^{1}H Spectroscopy and functional magnetic resonance imaging (fMRI) data were obtained at the same time using one interleaved scanning protocol. fMRI analysis, however, is not within the scope of this thesis. We started each scan session with a T1-weighted MR image for an anatomical overview of the brain (TR/TE= 4.2/1.87 s; field of view (FOV) = 246 × 246 x 180 mm; voxel size = 0.84 × 0.84 × 0.9 mm; slices = 200). Based on the T1-weighted image, a voxel of 18 × 18 × 25 mm was placed superior to the genu corporis callosi in the sagittal plane of the dACC for MRS (*Figure 5*), a region chosen for its involvement in stress-related cognitive processes and high population

of GABAerigc neurons. We adopted a semi-localization by adiabatic selective refocusing (sLA-SER) sequence (TR/TE = 3600/36 ms) and VAPOR water suppression (Boer et al., 2020), acquiring 64 spectra before, and 368 spectra after the stress intervention. Scans were designed to capture resting neural activity for which participants were instructed to look at a white cross in front of a black background.

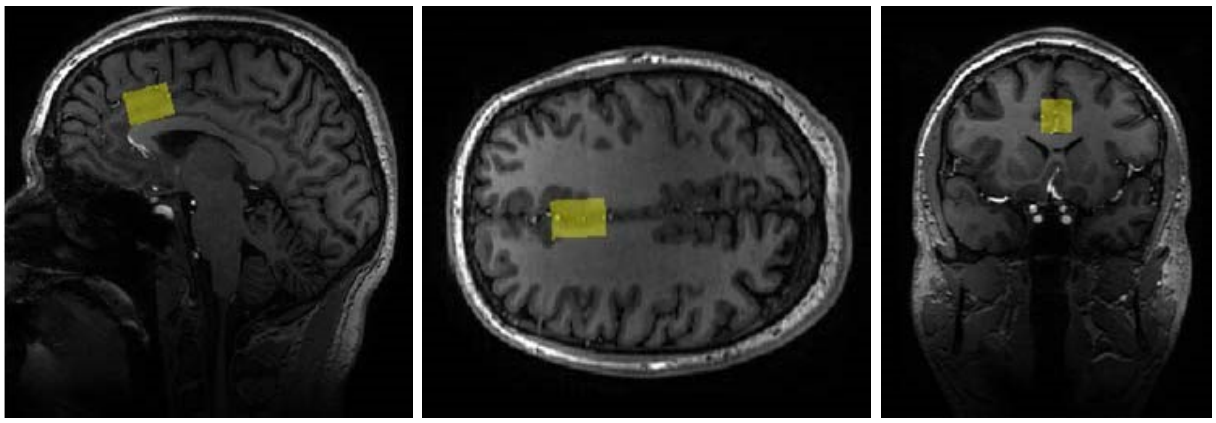

Figure 5 Voxel Placement. *Voxel was positioned superior to the genu corporis callosi in the sagittal plane of the dACC and validated in all three anatomical planes: sagittal (left), transverse (middle), coronal (right).*

4.6.2 MRS Data Processing

Prior to analysis of the spectra we performed several corrective steps using in-house developed MatLab (R2016a, Version 9.0.0.341360) scripts. The signal of each receiving channel were phase and amplitude corrected before coil combination. In a subsequent step, signal distortions caused by induction of electrical currents (eddy currents) by the magnetic field are removed using two unsuppressed water spectra. Individual spectra of one session were then phase and frequency corrected using spectral registration (Near et al., 2015), where the spectrum of highest quality is used as norm. The effects of eddy current correction (ECC) and spectral registration on signal to noise ratio (SNR) are depicted in *Figure 6.*

Metabolite concentrations were determined using LCModel (Version 6.3-1L) for a moving average of 64 spectra for all three scans. The tool LCModel scales reference signals of neurometabolites over the obtained full spectral image and returns a concentration of each reference metabolite based on its fitted area-under-the-curve value. Neurometabolites with a stable MRS signal, n-acteylaspertate, phosphocreatine, and phosphocholine were fitted first. In LC-Model

the confidence parameter %SD (standard deviation, in % of mean) is provided alongside the estimates for each concentration value, as well as the fitting curve of each reference signal (see *Figure 6d).* GABA and glutamate estimates with a %SD > 30 were omitted from analysis. Additionally, we excluded spectra with a SNR < 30 and a full-width half-maximum (FWHM) > 0.05.

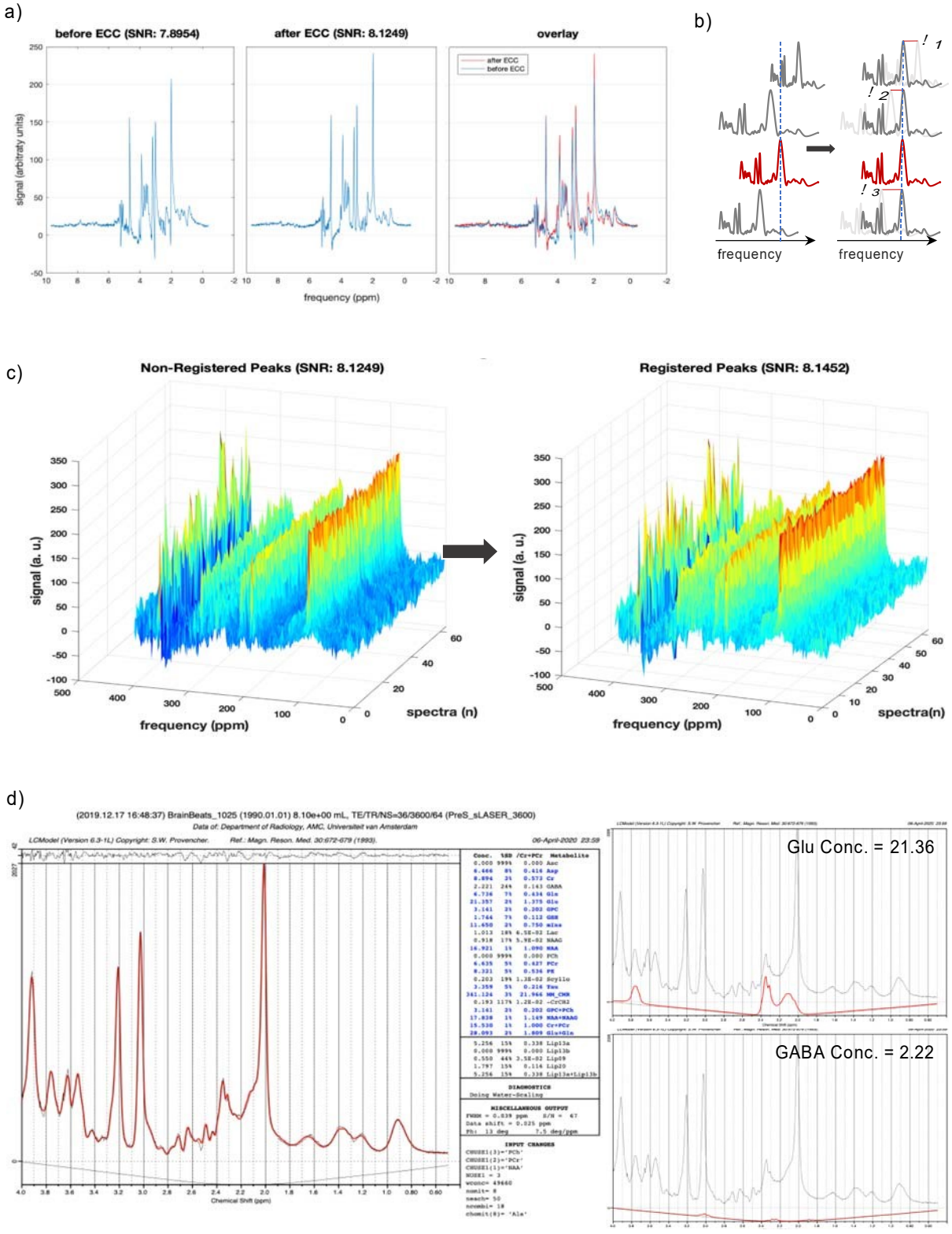

Figure 6 Processing pipeline of MRS spectra, participant 1025 - post-intervention. *(a) Metabolite spectrum before (left) and after (middle) eddy current correction (ECC). Eddy currents are common measuring artefacts induced by the scanner's magnetic field. Overlay (right) shows signal improvement after ECC marked by taller and narrower peaks. (b) schematic overview of spectral registration: spectra of one scan session (n=64) are aligned by shifts in frequency and phase in order to reduce distortions when summating the signal of multiple spectra. (c) Spectra of one scan session next to each other before (left) and*

after (right) spectral registration. The red peak band indicates noticeable improvement of the overall fit. (d) LC-Model software output of 64 spectral measurements (left). The program fits reference peaks of individual metabolites to the overall signal and determines a concentration. A concentration, confidence parameters (%SD, standard deviations in % of mean), as well as fitting curves (right) are provided.

4.7 Statistical Analysis

All statistical analyses were performed in R (version 3.6.3; R Core Team 2020) using General Linear Mixed-Effects Models with the function *lmer* of the lme4 package (Version 1.1-21; Bates, Mächler, Bolker, & Walker, 2015). Response variables were relativized to a baseline measurement prior to transformation, an overview of the full model syntaxes is given in *Table 1*. Fixed effect terms were assessed using likelihood-ratio tests (Barr, Levy, Scheepers, & Tily, 2013). *P*-values ≤ .05 were interpreted as significant.

Table 1 Response units and lmer function input for statistical modeling.

Response	**Units: x-fold of**	**Full Model**
Heart Rate	HR pre-intervention	$log_{10}(HR) \sim 1 + \ stress * phase \ + \ (1\|subID)$
Negative Affect	PANAS baseline score	$(-1) * \ PANAS_{neg}{}^{-1.4} \sim 1 + \ stress * session + \ (1\|subID)$ [1]
GABA	pre scan cGABA	$log_{10}(GABA) \sim 1 + \ scan + stress * time + \ (1 + m\_time + m\_scan \ \|subID)$
Glutamate	pre scan cGlu	$log_{10}(Glu) \sim 1 + \ scan + stress * time + (1 + m\_time + m\_scan \ \|subID)$

Explanatory Variables

subID: subject ID
stress: factor with levels 0 (control) and 1 (stress).
phase: factor with levels 0 (water) and 1 (arithmetic).
session: factor with levels 0 (pre-) and 1 (post-intervention).
scan: factor with levels 0 (Post1 scan) and 1 (Post2 scan).
m_scan: mean centered variable *scan*.
time: factor with 5 levels (0 – 4), each representing a time interval of 500 s (seconds), from 1000 s after stress onset onwards.
m_time: mean centered variable *time.*

[1] Tukey Ladder of Power Transformation (Tukey, 1977) using the function *transformTukey* from the rcompanion package (version 2.3.25, (Mangiafico, 2020)

4.7.1 Analysis of Heart Rate

We investigated the effects of stress on cardiac pulse and during two phases of the SECPT, the water task and the arithmetic task. *Stress* and *phase* were treated as fixed effects, *subjectID* was

included as a random effect to this model. Further, an interaction term of the fixed effects accounts for a possible disproportionate response to either task within one experimental group.

4.7.2 Analysis of Negative Affect

Negative affect, as determines by the Negative Affect Subscale of the PANAS, across stress and control group was compared before and after the intervention. For this, *stress*, *session*, and their interaction were included as fixed effects, *subjectID* as random effect in the model. Pre-intervention questionnaire scores were interpreted as response to the MRI scanner setting, changes in post-intervention questionnaire scores are attributed to the intervention itself. A difference in reactivity to the stress and control task is thus reflected in the model's estimate for the interaction term.

4.7.3 Analysis of Neurometabolite Data

GABA and glutamate responses were modelled in identical fashion. *Stress* and *time* were included as fixed effects in the model; where *time* is a factor with five levels, each representing a time interval of 500 s (seconds), from 1000 s after stress onset onwards. Their interaction accounts for group-specific neurotransmitter dynamics over time. In addition, a covariate of *scan* was considered by the model to avoid false positive time effects due to a baseline shift between the Post1 and Post2 scan. Collinearity between *time* and *scan* was ruled out by assessment of Variance Inflation Factors (Field, 2005) for a standard linear model excluding the random effects. The final model further fits random intercepts for *subjectID* and random slopes for *time* and *scan*, the latter two were mean centered before inclusion in the random effects term. For both glutamate and GABA modelling, the optimizer 'bobyqa' was used, and datapoints were weighed against their respective % SD values.

5. Results

5.1 Sample Characteristics

As shown in *Table 2*, stress and control group matched well in terms of age, IQ, PSS and drug/alcohol intake. For GABA and glutamate analysis, twelve (five control, seven stress) and two (both stress) participants had to be excluded due to insufficient data quality, respectively. Their exclusion had negligible effects on group demographics.

Table 2 Sample Characteristics. *Control and Stress group did not differ significantly in matching criteria.*

Matching Criterion	Control, M (SD)	Stress, M (SD)	t-statistic, *p*	Total, M (SD)
Age (years)	24.3 (3.03)	24.1 (2.67)	0.784	24.2 (2.84)
IQ	100.82 (7.84)	100.54 (6.15)	0.882	100.54 (7.04)
PSS	8.46 (3.81)	9.04 (4.37)	0.611	8.75 (4.11)
AUDIT	5.11 (3.26)	5.18 (2.69)	0.93	5.14 (2.98)
DUDIT	1.68 (2.24)	1.39 (1.95)	0.619	1.54 (2.1)

5.2 Cardiac Parameters

There were no detectable changes between pre- and post-intervention ECGs for any of the participants. In terms of heart rate, we recorded a mean increase of 5% during the water task and a mean 10% increase during the arithmetic task; the response of stressed and unstressed individuals was comparable. And although the arithmetic task evoked a slightly stronger response in the stress group, the overall effect of stress is insignificant ($\chi^2 = 3.11$, df = 2, p = 0.211). Individual heart responses to the stress paradigm ranged from very weak to strong, as is demonstrated in *Figure 7*. Whereas some participants barely reacted to the cold water, others showed an increase in heart rate of 20 %.

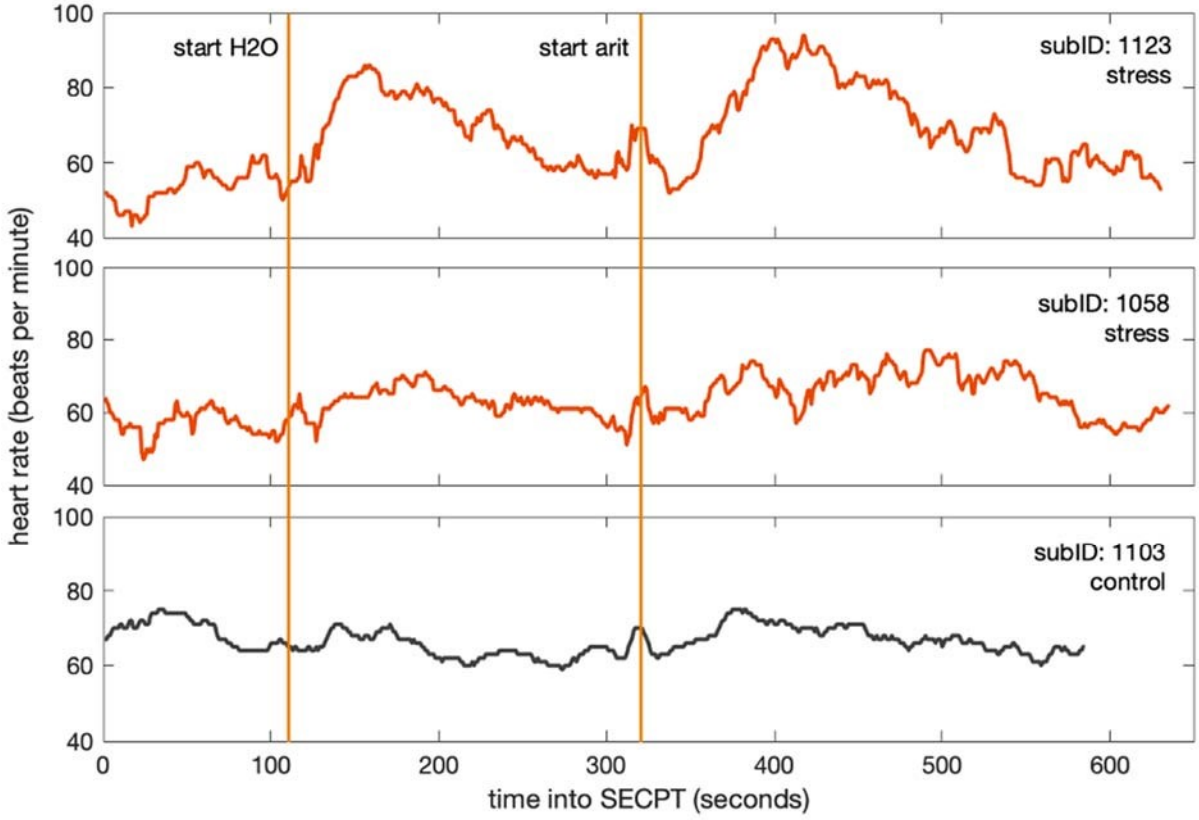

Figure 7 Comparison of Heart Response between Subjects. *Heart rate is depicted for three individuals (two stressed, one control) during the SECPT, the start of the water and arithmetic tasks are indicated on the graphs. Cardiac response to stress varied immensely between individuals. Subject 1123 reacted strongly to both tasks, subject 1058 shows little response overall, as does subject 1103 of the control group. Data noise differs greatly between recordings.*

5.3 Negative Affect Scores

Baseline PANAS scores were examined in a Wilcoxon Mann-Whitney Rank Sum Test and reveal similar negative affect between stress (mean = 14. 96, SD = 2. 22) and control (mean = 16.36, SD = 3.96) subjects at their arrival to the facility (W = 303.5, p = .134). Both experimental groups showed a reduction in negative affect at the start of scanning (pre-intervention) of about 20 %.

Comparison with the null model suggests a strong overall impact of the fixed effects *stress* and *session* ($\chi^2 = 27.84$, df = 3, $p < .001$). More specifically, we observed a clear difference between stress and control group in their reactions to the intervention ($t(56) = 4.267$, $p < .001$): while negative affect score decreased by another 11 % for controls ($p < .001$), it remained unchanged for subjects of the stress group ($t(56) = -1.092$, $p = .696$) (*Figure 8*). These results indicate that

controls gradually acclimatized to the testing environment, whereas the SECPT arrested this process in stressed individuals.

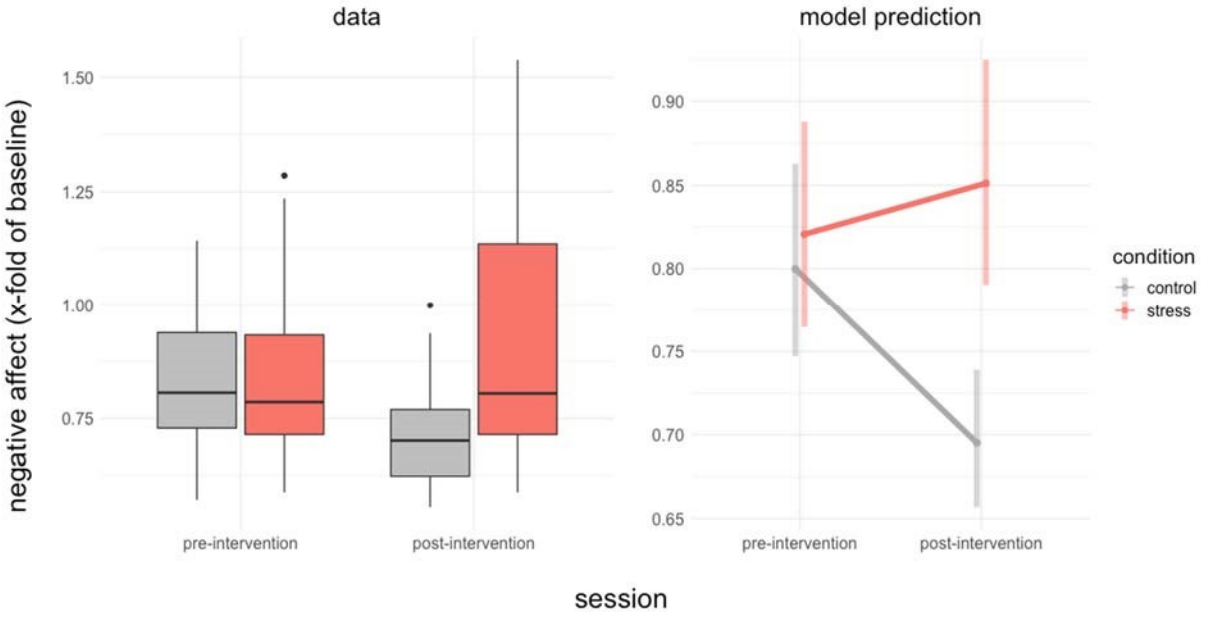

Figure 8 Effect of Intervention on Negative Affect. *Comparison of pre- and post-intervention responses between stress and control group (both n = 28) (left) and estimates by linear mixed-effects model (right). Values are relative to baseline score sampled at the arrival of each participant. Estimates are depicted with their respective confidence intervals of size 0.95, overlapping confidence intervals of two estimates implies non-significance.*

5.4 Neurometabolite Evaluation

5.4.1 GABA Concentration Changes over Time

Overall quality of GABA measurements was poor, 46 % of all data points had to be excluded from analysis. *Figure 9a* shows the change of GABA concentration over time for each experimental group. While not true for all participants, controls in general showed more stable metabolite concentrations.

Comparison with the null model suggests an overall strong impact of fixed effects ($\chi^2 = 254.33$, df = 10, $p < .001$), this can largely be attributed to changes in time. Specifically, both stress ($t(72.3) = -5.956$, $p < .001$) and control group ($t(70) = -4.374$, $p = .002$) show an increase in GABA between time intervals 0 and 1. The statistical model predicts slightly lower GABA concentrations for controls in earlier timepoints than for stressed individuals, however these differences fall below the significance threshold. Experimental group therefore did not considerably modulate GABA response. This is shown in Figure *9b*.

We further investigated the effect of scan session on our measurements. For GABA, we found no difference in recordings between the first and second post-intervention scans. The covariate was not omitted from the model, as it did have a strong impact on glutamate results (see below).

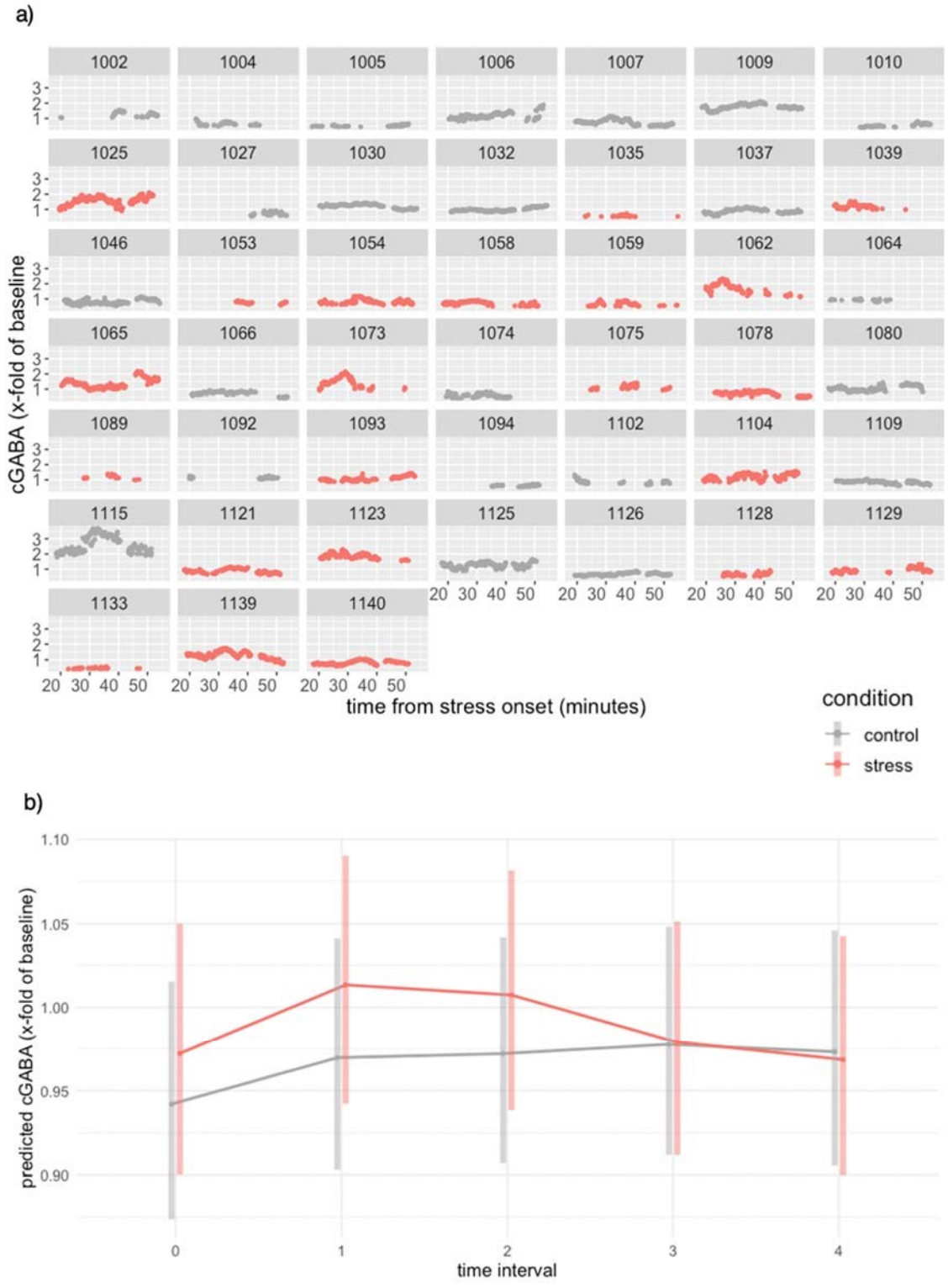

Figure 9 Effect of Intervention on Prefrontal GABA Concentration. *GABA response between stress (n = 22) and control (n = 24) group. (a) Per participant metabolite concentrations in minutes from stress onset, relativized to a baseline level. Low data quality results in large gaps between individual measuring points. Reaction patterns between experimental groups are not discernible. (b) Predicted GABA responses for each experimental group by lmer model with their respective confidence intervals of 0.95, overlapping confidence intervals of two estimates implies non-significance. Each time interval represents a period of 500 seconds, from 1000 seconds after stress onset onwards.*

5.4.2 Glutamate Concentration Changes over Time

Quality filtering of spectra resulted in a loss of 3 % of all glutamate data points. *Figure 10a* shows each participant's glutamate response over time. For all participants, glutamate levels remained stable for the duration of the post-intervention measurement. Glutamate concentrations of two participants were remarkably elevated in regard to the baseline measurement. Statistical modelling confirms stress had no influence on prefrontal glutamate response. Model estimates for different timepoints and experimental groups are indistinguishable considering their relatively large confidence intervals. We noticed measurements of the second post-intervention scan were systemically higher, about 1 %, for both groups ($t(57.0) = -3.452$, $p = .006$) at the average timepoint. This suggests scan to be an important covariate to the model, as differences in metabolite concentrations might otherwise be attributed to time.

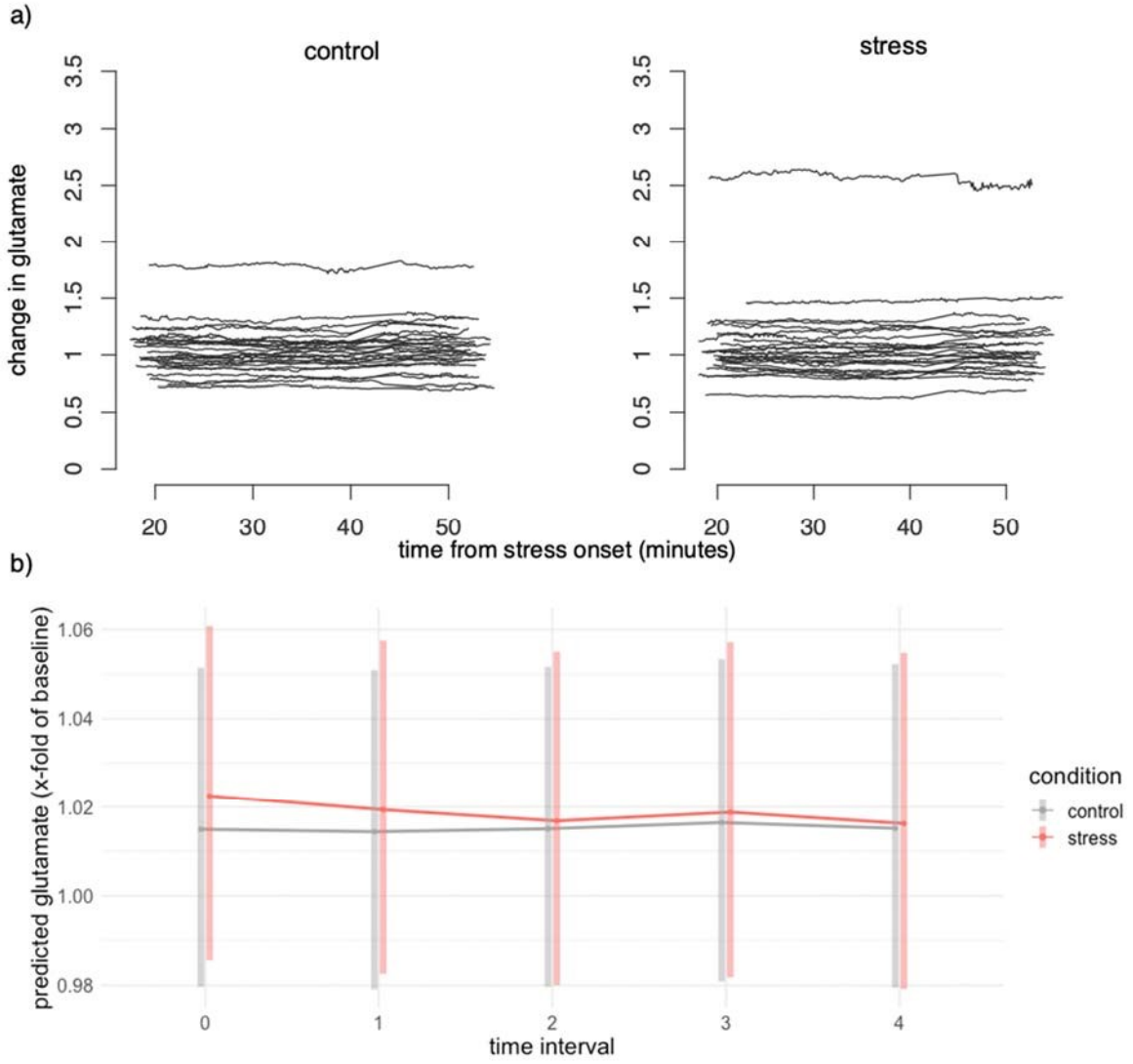

Figure 10 Effect of Intervention on Prefrontal Glutamate Concentration. *Glutamate response between stress (n = 26) and control (n = 28) group. (a) Metabolite concentrations remain stable over time (in minutes from stress onset) for both groups. The baseline shift at t = 42 minutes between first and second scanning session is clearly visible. (b) Predicted glutamate response over the same intervals by statistical modeling with their respective confidence intervals of 0.95, overlapping confidence intervals of two estimates implies non-significance. Each time interval represents a period of 500 seconds, from 1000 seconds after stress onset onwards.*

6. Discussion

To better understand the regulation of dACC and autonomic activity in stress, we investigated the changes in prefrontal GABA and glutamate concentrations in response to acute stress. GABA and glutamate concentrations in the dACC were measured in the time interval of 18-55 minutes after stress onset and compared to participants' heart rate during the SECPT. Additionally, self-reported questionnaires were acquired throughout the scan procedure to assess subjective stress levels.

Success of stress induction with the SECPT is commonly determined through respective measurement of psychological, endocrine, and autonomic indicators (Schwabe et al., 2008). On a group level, stressed individuals reported higher negative affect scores than controls, but there was no significant difference in heart rate response. On the individual level, stress reactivity is measured in terms of cortisol response, as reliable thresholds for HPA arousal have previously been established (Miller, Plessow, Kirschbaum, & Stalder, 2013). However, due to time restrictions, salivary cortisol samples have not yet been analyzed. With these results at hand, we cannot make a clear verdict on the success of our stress induction paradigm and it is important to revisit this question in its full context once data on cortisol is available. This importance is highlighted in a meta-analysis of studies involving the SECPT, which showed positive response rate to the paradigm, as assessed in terms of cortisol response, ranged from 48 to 84 percent between studies (Schwabe & Schächinger, 2018). The possibility of non-responders being overrepresented in the stress group thus needs to be evaluated.

While the effects of stress on heart rate are well known, there have been different reports regarding heart rate behavior in response to the SECPT specifically: heart rate has been shown to increase (Giles, Mahoney, Brunyé, Taylor, & Kanarek, 2014), as well as to not react (Schwabe et al., 2008) in response to the SECPT, and may therefore not be a reliable stress indicator for this task. This might be due to the cold water component, which has been speculated to evoke an increase in blood pressure that counteracts the regular heart rate increase during stress through activation of the baroreflex (Schwabe & Schächinger, 2018). While this provides a possible explanation to our negative findings in cardiac response, it also provides an incentive

to explore different parameters. Heart rate variability (HRV) is one of such which compares the millisecond variation of inter-beat intervals in a given time interval (Task Force of the European Society Electrophysiology, 1996). Effects of stress on HRV are also well documented (A. Hernando et al., 2016; D. Hernando, Roca, Sancho, Alesanco, & Bailón, 2018; Kim, Cheon, Bai, Lee, & Koo, 2018) and may potentially be less sensitive to specificities of the SECPT. A follow-up analysis will thus be conducted. Analysis of HRV will be of particular relevance, since also no changes in participants' ECGs were observed. This, however, is most likely due to the time interval between stress onset and post-intervention ECG being too long to detect autonomic modulation (t ~ 60 minutes).

We were not able to determine a significant difference between stress and control group in terms of dACC GABA modulation. This goes against the notion that GABA is a key regulator in the stress response, however, data loss was a critical issue in this analysis. The exclusion of twelve participants inevitably reduced statistical power and thus sensitivity in detecting group differences. A small group effect might have therefore gone unnoticed. GABA concentrations, albeit insignificantly, were observed to be higher in stressed individuals compared to controls in the first three time intervals of recording. Interestingly, this goes against previous associations of prefrontal GABA decreases with CNS stress behavior (Hasler et al., 2010). One noticeable difference to our study is the timing of MRS relative to stress onset, as Hasler's research group (2010) conducted their measurements during a stress task, not afterwards. A second study investigated the response of GABA approximately 30 minutes after stress induction was also not able to find an effect (Houtepen et al., 2017). Taken together, these results hint towards a narrow timeframe of GABA-mediated SN activation in response to stress. Indeed, SN activity in acute stress is known gradually to subside in favor of CEN-mediated processing (Hermans et al., 2014), the exact timeline of this adaptation has not yet been investigated. We show that these adaptations occur in a glutamate-independent manner, and that further clarification regarding the role of GABA is necessary. MRS data will be evaluated in the context of fMRI at a later point in time, where the activity of SN- and CEN-specific domains can be correlated to our neurometabolite measurements.

These preliminary findings urge more elaborate analysis of the whole experiment, but nonetheless raise interesting questions for debate. Stress responsiveness, cortisol and autonomic measures still need to be verified, and spectroscopic measurements put into context with fMRI data analysis. Several limitations to these results have been pointed out. We did not find a link between prefrontal GABA concentrations and stress and, moreover, cardiac response, however wish to critically reassess these findings in their full context.

Summary

The human stress response is a systemic effort to maintain homeostatic balance under real, perceived, or anticipated threat. In the periphery, its effects are mediated by the autonomic nervous system (ANS) and bloodstream cortisol, end product of the hypothalamus-pituitary-adrenocortical axis (HPA). All is overseen by a central nervous regulatory component, which adjusts the intensity and duration of peripheral response and integrates peripheral signals of stress into higher-order cognitive and behavioral processes. A dysregulation of this complex system (through prolonged or over-intensive exposure to stress) can have devastating effects on mental and physical health, including cardiac health. For example, periods of severe acute stress have been linked to cardiac arrythmias and can even lead to sudden cardiac death (SCD), possibly due to a disruption in ANS control of the heart.

The importance of prefronto-limbic structures such as the dorsal anterior cingulate cortex (dACC) and γ-aminobutyric acid (GABA) pathways in stress regulation is widely recognized. GABA-receptor antagonists such as bicuculline are categorized as anxiogenic, whereas GABA-receptor agonistic medication such as members of the benzodiazepine family are commonly prescribed for their anxiolytic effects. Consistent with these insights, a previous magnetic resonance spectroscopy (MRS) study has shown prefrontal GABA concentrations to decrease in immediate response to stress. Moreover, recent reports confirm sudden discontinuation of GABA-receptor agonistic medication can result in development of cardiomyopathy clinically indistinguishable from SCD.

The present study extends this research by investigating possible correlates between prefrontal GABA concentrations and cardiac markers. Fifty-six psychologically and physically healthy males (mean age = 24.18) were included in a between-subject experimental setup to investigate GABA and glutamate response in the dACC to a well-established stress task (i.e. the Socially Evaluated Cold Pressor Task). We adopted a semi-localization by adiabatic selective refocusing (sLASER) measuring sequence (TR/TE = 3600/36 ms) at ultra-high field 7T MRS, acquiring 64 spectra before, and 368 spectra after the stress intervention in a task-negative setting. Additionally, salivary cortisol content and electrocardiographic (ECG) markers of participants were measured to determine HPA and ANS activation, respectively. Spectroscopy and ECG data was

analyzed in the same context to explore the possibility of temporal dependencies between the two and assessed for reliable measures of stress vulnerability.

We did make out a significant difference between stress and control group in terms of dACC GABA modulation. This goes against the notion that GABA is a key regulator in the stress response, however, data loss was a critical issue in this analysis. Reduced statistical power might leave small effects unnoticed and as a next step we will validate our findings with functional magnetic resonance imaging datasets. Furthermore, we found the stress task to have no effect on ECG parameters, and we raise the question of its suitability to measure SAM activation in the paradigm at hand. Due to timely restrictions, salivary cortisol data could not be included in the analysis; HPA and SAM activation will have to be addressed at a later point again.

Zusammenfassung

Die Stressantwort im Menschen ist eine systemische Anstrengung der Erhaltung homöostatischen Gleichgewichts unter realer, wahrgenommener oder antizipierter Gefahr. In der Peripherie wird sie durch das autonome Nervensystem (ANS) und durch zirkulierendes Cortisol, dem Endprodukt der Hypothalamus-Hypophysen-Nebennierenrinden-Achse (HPA), vermittelt. Das zentrale Nervensystem übernimmt hierbei die Regulation der Intensität und Dauer der peripheren Reaktion und integriert zudem Stresssignale in kognitive Prozesse und das Verhalten. Eine Maladaption dieses komplexen Systems (etwa durch chronische oder überintensive Belastung) kann verheerende Auswirkungen auf geistige und körperliche Gesundheit - einschließlich der des Herzens - haben. So wurden stresslastige Lebensperioden mit Herzrhythmusstörungen in Verbindung gebracht und können in seltenen Fällen zu plötzlichem Herztod (SCD) führen, möglicherweise wegen einer Störung ANS-bedingter Regulationsmechanismen.
Die Bedeutung präfronto-limbischer Strukturen wie dem dorsalen *cortex cingularis anterior* (dACC) und γ-Aminobuttersäure-(GABA)-erger Neuronen in der Stressregulation ist weit anerkannt. GABA-Rezeptor-Antagonisten wie Bicucullin werden als anxiogen eingestuft, während GABA-Rezeptor-agonistische Medikamente, wie etwa Mitglieder der Benzodiazepin-Familie, üblicherweise für ihre anxiolytische Wirkung verschrieben werden. In Übereinstimmung mit diesen Erkenntnissen hat eine Magnetresonanzspektroskopie-Studie (MRS) bereits gezeigt, dass die präfrontalen GABA-Konzentrationen in unmittelbarer Reaktion auf Stress abnehmen. Darüber hinaus bestätigen neuere Berichte, dass ein plötzliches Absetzen GABA-Rezeptor-agonistischer Medikamente zur Entwicklung einer Kardiomyopathie führen kann, die klinisch von SCD nicht zu unterscheiden ist.

Mit diesem Hintergrund wurde in der vorliegenden Studie der Zusammenhang präfrontaler GABA-Konzentrationen und Herzparametern untersucht. Hierfür wurden 56 psychisch und physisch gesunde Männer (Durchschnittsalter = 24,18 Jahre) einem gängigen Stressparadigma (dem *Socially Evaluated Cold Pressor Task*) unterzogen, und anschließend mittels 7T MRS deren GABA- und Glutamatgehalt im dACC gemessen. Wir bedienten uns einer *semi-localization by adiabatic selective refocusing* (sLASER) Messsequenz (TR / TE = 3600/36 ms), wobei

64 Spektra vor, und 368 Spektra nach der Stressintervention in einem aufgabennegativen Umfeld aufgenommen wurden. Zusätzlich wurden Cortisolgehalt im Speichel und elektrokardiographische (ECG) Marker der Teilnehmer ermittelt, um das Ausmaß einer HPA- bzw. ANS-Aktivierung zu bestimmen. Spektroskopie- und ECG-Daten wurden im selben Kontext analysiert, um die Möglichkeit zeitlicher Abhängigkeiten zu untersuchen, und um diese als Parameter für die Stressempfindlichkeit zu evaluieren.

Wir stellten wider anfänglicher Annahme keine Unterschiede zwischen Stress- und Kontrollgruppe in Hinblick präfrontaler GABA-Konzentrationen fest, jedoch hatten wir in dieser Analyse mit kritischen Datenverlusten umzugehen. Die verringerte Aussagekraft unsere Auswertung könnte kleine Effekte außer Acht lassen, eine Validierung unserer Ergebnisse mit funktioneller Magnetresonanz-Datensätze ist im nächsten Schritt daher von besonderer Bedeutung. Wir zeichneten ebenfalls keinen Effekt von Stress auf ECG-Parameter auf, und wir hinterfragen die Eignung dieser zur Messung von SAM-Aktivierung in dem vorliegenden experimentellen Kontext. Aufgrund zeitlicher Einschränkungen war der Cortisol-Datensatz nicht Teil der Analyse; HPA- und SAM-Aktivität müssen zu einem späteren Zeitpunkt nochmals eruiert werden.

Abbreviations

ANS	Autonomic Nervous System
arit	arithmetic task of the SECPT
AUDIT	Alcohol Use Disorders Identification Test
B_0	external magnetic field
CEN	central executive network
CNS	Central Nervous System
dACC	dorsal anterior cingulate cortex
df	degrees of freedom
DMN	default mode network
DUDIT	Drug Use Disorders Identification Test
ECC	eddy current correction
ECG	electrocardiogram
FWHM	full-width half-maximum
GABA	γ-aminobutyric acid
^1H	protium, most prevalent hydrogen isotope
H_2O	water task of the SECPT
HPA	hypothalamus-pituitary-adrenocortical axis
HR	heart rate
HRV	heart rate variability
IQ	intelligence quotient
M	mean
M	net magnetization of sample (Section 2. Technical Background)
m	minutes
mPFC	medial prefrontal cortex
MRI, fMRI	(functional) magnetic resonance imaging
MRS	magnetic resonance spectroscopy
n	sample size
NTS	nucleus of the solitary tract
PANAS-SF	Positive and Negative Affect Schedule, short form

ppm	parts per million, 10^{-6}
PSS	Perceived Stress Scale
PVN	paraventricular nucleus of the hypothalamus
RF	radiofrequency
SAM	sympatho-adrenomedullary axis
SCD	sudden cardiac death
SD	standard deviation
%SD	standard deviation, in % of mean
SECPT	Socially Evaluated Cold Pressure Task
sLASER	semi- localization by adiabatic selective refocusing
SNR	signal-to-noise ratio
SN	salience network
s	seconds
t(df)	t-statistic
TE	time of echo
TR	time of repetition
T	Tesla
χ^2	chi-squared statistic

Support

Statistical analysis was closely guided by the biostatistical platform of the University of Veterinary Medicine in Vienna. I would like to express my gratitude to Dr. Marlies Dolezal in particular, who has generously offered her expertise on the subject, at times well out-of-office hours.

Tables and Figures

References

Andrews-Hanna, J. R., Reidler, J. S., Sepulcre, J., Poulin, R., & Buckner, R. L. (2010). Functional-anatomic fractionation of the brain's default network. *Neuron*, *65*(4), 550–562. https://doi.org/10.1016/j.neuron.2010.02.005

Barr, D. J., Levy, R., Scheepers, C., & Tily, H. J. (2013). Random effects structure for confirmatory hypothesis testing: Keep it maximal. *Journal of Memory and Language*, *68*(3), 255–278. https://doi.org/10.1016/j.jml.2012.11.001

Bates, D., Mächler, M., Bolker, B., & Walker, S. (2015). Fitting Linear Mixed-Effects Models Using lme4. *Journal of Statistical Software*, *67*(1). https://doi.org/10.18637/jss.v067.i01

Beck, A. T., Steer, R. A., & Brown, G. K. (1996). Manual for the Beck depression inventory-II. In *San Antonio, TX: Psychological Corporation*. San Antonio, TX.

Berman, A., Bergman, H., Palmstierna, T., & Schlyter, F. (2003). *DUDIT-The Drug Use disorder identification test*.

Bertholdo, D., Watcharakorn, A., & Castillo, M. (2013). Brain Proton Magnetic Resonance Spectroscopy. *Neuroimaging Clinics of North America*, *23*(3), 359–380. https://doi.org/10.1016/j.nic.2012.10.002

Boer, V. O., Andersen, M., Lind, A., Lee, N. G., Marsman, A., & Petersen, E. T. (2020). MR spectroscopy using static higher order shimming with dynamic linear terms (HOS-DLT) for improved water suppression, interleaved MRS-fMRI, and navigator-based motion correction at 7T. *Magnetic Resonance in Medicine*, *n/a*(n/a). https://doi.org/10.1002/mrm.28202

Bottomley, P. A. (1987). Spatial Localization in NMR Spectroscopy in Vivo. *Annals of the New York Academy of Sciences*, *508*(1 Physiological), 333–348. https://doi.org/10.1111/j.1749-6632.1987.tb32915.x

Chen, C., Sigurdsson, H. P., Pépés, S. E., Auer, D. P., Morris, P. G., Morgan, P. S., … Jackson, S. R. (2017). Activation induced changes in GABA: Functional MRS at 7 T with MEGA-sLASER. *NeuroImage*, *156*, 207–213. https://doi.org/10.1016/J.NEUROIMAGE.2017.05.044

Chrousos, G. P., & Gold, P. W. (1992). The Concepts of Stress and Stress System Disorders: Overview of Physical and Behavioral Homeostasis. *JAMA: The Journal of the American*

Medical Association, *267*(9), 1244–1252. https://doi.org/10.1001/jama.1992.03480090092034

Cohen, S., Kamarck, T., & Mermelstein, R. (1983). A Global Measure of Perceived Stress. *Journal of Health and Social Behavior*, *24*(4), 385. https://doi.org/10.2307/2136404

Cohen, S., Tyrrell, D. A. J., & Smith, A. P. (1991). Psychological Stress and Susceptibility to the Common Cold. *New England Journal of Medicine*, *325*(9), 606–612. https://doi.org/10.1056/NEJM199108293250903

Cole, S. W., Hawkley, L. C., Arevalo, J. M., Sung, C. Y., Rose, R. M., & Cacioppo, J. T. (2007). Social regulation of gene expression in human leukocytes. *Genome Biology*, *8*(9). https://doi.org/10.1186/gb-2007-8-9-r189

Corbetta, M., Patel, G., & Shulman, G. L. (2008). The Reorienting System of the Human Brain: From Environment to Theory of Mind. *Neuron*, *58*(3), 306–324. https://doi.org/https://doi.org/10.1016/j.neuron.2008.04.017

Courtin, J., Chaudun, F., Rozeske, R. R., Karalis, N., Gonzalez-Campo, C., Wurtz, H., … Herry, C. (2014). Prefrontal parvalbumin interneurons shape neuronal activity to drive fear expression. *Nature*, *505*(7481), 92–96. https://doi.org/10.1038/nature12755

Cunningham, E. T., Bohn, M. C., & Sawchenko, P. E. (1990). Organization of adrenergic inputs to the paraventricular and supraoptic nuclei of the hypothalamus in the rat. *The Journal of Comparative Neurology*, *292*(4), 651–667. https://doi.org/10.1002/cne.902920413

Cuypers, K., Verstraelen, S., Maes, C., Hermans, L., Hehl, M., Heise, K.-F., … Swinnen, S. P. (2020). Task-related measures of short-interval intracortical inhibition and GABA levels in healthy young and older adults: A multimodal TMS-MRS study. *NeuroImage*, *208*, 116470. https://doi.org/10.1016/j.neuroimage.2019.116470

Day, R., Nielsen, J. A., Korten, A., Ernberg, G., Dube, K. C., Gebhart, J., … Wynne, L. C. (1987). Stressful life events preceding the acute onset of schizophrenia: A cross-national study from the World Health Organization. *Culture, Medicine and Psychiatry*, *11*(2), 123–205. https://doi.org/10.1007/BF00122563

de Graaf, R. A. (2019). *in vivo NMR Spectroscopy - Principles and Techniques* (3rd ed.). Hoboken, NJ: John Wiley & Sons Ltd.

Delli Pizzi, S., Chiacchiaretta, P., Mantini, D., Bubbico, G., Edden, R. A., Onofrj, M., … Bonanni, L. (2017). GABA content within medial prefrontal cortex predicts the variability

of fronto-limbic effective connectivity. *Brain Structure and Function*, *222*(7), 3217–3229. https://doi.org/10.1007/s00429-017-1399-x

Droste, S. K., de Groote, L., Atkinson, H. C., Lightman, S. L., Reul, J. M. H. M., & Linthorst, A. C. E. (2008). Corticosterone Levels in the Brain Show a Distinct Ultradian Rhythm but a Delayed Response to Forced Swim Stress. *Endocrinology*, *149*(7), 3244–3253. https://doi.org/10.1210/en.2008-0103

Ellard, K. K., Barlow, D. H., Whitfield-Gabrieli, S., Gabrieli, J. D. E., & Deckersbach, T. (2017). Neural correlates of emotion acceptance vs worry or suppression in generalized anxiety disorder. *Social Cognitive and Affective Neuroscience*, *12*(6), 1009–1021. https://doi.org/10.1093/scan/nsx025

Felmlee, J. P., & Ehman, R. L. (1987). Spatial presaturation: a method for suppressing flow artifacts and improving depiction of vascular anatomy in MR imaging. *Radiology*, *164*(2), 559–564. https://doi.org/10.1148/radiology.164.2.3602402

Fransson, P., & Marrelec, G. (2008). The precuneus/posterior cingulate cortex plays a pivotal role in the default mode network: Evidence from a partial correlation network analysis. *NeuroImage*, *42*(3), 1178–1184. https://doi.org/https://doi.org/10.1016/j.neuroimage.2008.05.059

Garnefski, N., & Kraaij, V. (2001). Levensgebeurtenissen Vragenlijst.

Giles, G. E., Mahoney, C. R., Brunyé, T. T., Taylor, H. A., & Kanarek, R. B. (2014). Stress effects on mood, HPA axis, and autonomic response: Comparison of three psychosocial stress paradigms. *PLoS ONE*, *9*(12), 1–19. https://doi.org/10.1371/journal.pone.0113618

Goldberg, A. D., Becker, L. C., Bonsall, R., Cohen, J. D., Ketterer, M. W., Kaufman, P. G., … Sheps, D. S. (1996). Ischemic, Hemodynamic, and Neurohormonal Responses to Mental and Exercise Stress. *Circulation*, *94*(10), 2402–2409. https://doi.org/10.1161/01.CIR.94.10.2402

Gottdiener, J. S., Krantz, D. S., Howell, R. H., Hecht, G. M., Klein, J., Falconer, J. J., & Rozanski, A. (1994). Induction of silent myocardial ischemia with mental stress testing: Relation to the triggers of ischemia during daily life activities to ischemic functional severity. *Journal of the American College of Cardiology*, *24*(7), 1645–1651. https://doi.org/10.1016/0735-1097(94)90169-4

Hasler, G., van der Veen, J. W., Grillon, C., Drevets, W. C., & Shen, J. (2010). Effect of acute

psychological stress on prefrontal GABA concentration determined by proton magnetic resonance spectroscopy. *The American Journal of Psychiatry*, *167*(10), 1226–1231. https://doi.org/10.1176/appi.ajp.2010.09070994

Herman, J. P., Figueiredo, H., Mueller, N. K., Ulrich-Lai, Y., Ostrander, M. M., Choi, D. C., & Cullinan, W. E. (2003). Central mechanisms of stress integration: hierarchical circuitry controlling hypothalamo–pituitary–adrenocortical responsiveness. *Frontiers in Neuroendocrinology*, *24*(3), 151–180. https://doi.org/10.1016/J.YFRNE.2003.07.001

Hermans, E. J., Henckens, M. J. A. G., Joëls, M., & Fernández, G. (2014). Dynamic adaptation of large-scale brain networks in response to acute stressors. *Trends in Neurosciences*, *37*(6), 304–314. https://doi.org/10.1016/j.tins.2014.03.006

Hernando, A., Lazaro, J., Gil, E., Arza, A., Garzon, J. M., Lopez-Anton, R., … Bailon, R. (2016). Inclusion of Respiratory Frequency Information in Heart Rate Variability Analysis for Stress Assessment. *IEEE Journal of Biomedical and Health Informatics*, *20*(4), 1016–1025. https://doi.org/10.1109/JBHI.2016.2553578

Hernando, D., Roca, S., Sancho, J., Alesanco, Á., & Bailón, R. (2018). Validation of the Apple Watch for Heart Rate Variability Measurements during Relax and Mental Stress in Healthy Subjects. *Sensors*, *18*(8), 2619. https://doi.org/10.3390/s18082619

Houtepen, L. C., Schür, R. R., Wijnen, J. P., Boer, V. O., Boks, M. P. M., Kahn, R. S., … Vinkers, C. H. (2017). Acute stress effects on GABA and glutamate levels in the prefrontal cortex: A 7T 1H magnetic resonance spectroscopy study. *NeuroImage: Clinical*, *14*, 195–200. https://doi.org/10.1016/J.NICL.2017.01.001

Kendler, K. S., Karkowski, L. M., & Prescott, C. A. (1999). Causal relationship between stressful life events and the onset of major depression. *American Journal of Psychiatry*, *156*(6), 837–841. https://doi.org/10.1176/ajp.156.6.837

Kim, H.-G., Cheon, E.-J., Bai, D.-S., Lee, Y. H., & Koo, B.-H. (2018). Stress and Heart Rate Variability: A Meta-Analysis and Review of the Literature. *Psychiatry Investigation*, *15*(3), 235–245. https://doi.org/10.30773/pi.2017.08.17

Koric, L., Volle, E., Seassau, M., Bernard, F. A., Mancini, J., Dubois, B., … Levy, R. (2012). How cognitive performance-induced stress can influence right VLPFC activation: An fMRI study in healthy subjects and in patients with social phobia. *Human Brain Mapping*, *33*(8), 1973–1986. https://doi.org/10.1002/hbm.21340

Lee, S., Yoon, B. E., Berglund, K., Oh, S. J., Park, H., Shin, H. S., … Lee, C. J. (2010). Channel-mediated tonic GABA release from glia. *Science*, *330*(6005), 790–796. https://doi.org/10.1126/science.1184334

Levy, J., De Brier, G., Hugeron, C., Lansaman, T., & Bensmail, D. (2016). Takotsubo cardiomyopathy as a reversible complication of intrathecal baclofen withdrawal. *Annals of Physical and Rehabilitation Medicine*, *59*(5–6), 340–342. https://doi.org/10.1016/j.rehab.2016.07.384

Mangiafico, S. S. (2020). Summary and Analysis of Extension Program Evaluation in R, version 2.3.25. Retrieved from rcompanion.org/handbook/

Marteau, T. M., & Bekker, H. (1992). The development of a six-item short-form of the state scale of the Spielberger State—Trait Anxiety Inventory (STAI). *British Journal of Clinical Psychology*, *31*(3), 301–306. https://doi.org/10.1111/j.2044-8260.1992.tb00997.x

McEwen, B. S. (2000). Allostasis and allostatic load: Implications for neuropsychopharmacology. *Neuropsychopharmacology*, *22*(2), 108–124. https://doi.org/10.1016/S0893-133X(99)00129-3

Mescher, M., Merkle, H., Kirsch, J., Garwood, M., & Gruetter, R. (1998). Simultaneousin vivo spectral editing and water suppression. *NMR in Biomedicine*, *11*(6), 266–272. https://doi.org/10.1002/(SICI)1099-1492(199810)11:6<266::AID-NBM530>3.0.CO;2-J

Miller, R., Plessow, F., Kirschbaum, C., & Stalder, T. (2013). Classification criteria for distinguishing cortisol responders from nonresponders to psychosocial stress: Evaluation of salivary cortisol pulse detection in panel designs. *Psychosomatic Medicine*, *75*(9), 832–840. https://doi.org/10.1097/PSY.0000000000000002

Murphy, E. A., Davis, J. M., Carmichael, M. D., Gangemi, J. D., Ghaffar, A., & Mayer, E. P. (2008). Exercise stress increases susceptibility to influenza infection. *Brain, Behavior, and Immunity*, *22*(8), 1152–1155. https://doi.org/10.1016/J.BBI.2008.06.004

Near, J., Edden, R., Evans, C., Paquin, R., Harris, A., & Jezzard, P. (2015). Frequency and Phase Drift Correction of Magnetic Resonance Spectroscopy Data by Spectral Registration in the Time Domain. *Magnetic Resonance in Medicine : Official Journal of the Society of Magnetic Resonance in Medicine / Society of Magnetic Resonance in Medicine*, *73*. https://doi.org/10.1002/mrm.25094

Prasad, A., Lerman, A., & Rihal, C. S. (2008). Apical ballooning syndrome (Tako-Tsubo or

stress cardiomyopathy): A mimic of acute myocardial infarction. *American Heart Journal*, *155*(3), 408–417. https://doi.org/10.1016/J.AHJ.2007.11.008

Preece, N. E., & Cerdán, S. (2002). Metabolic Precursors and Compartmentation of Cerebral GABA in Vigabatrin-Treated Rats. *Journal of Neurochemistry*, *67*(4), 1718–1725. https://doi.org/10.1046/j.1471-4159.1996.67041718.x

Purves, D. (2018). *Neuroscience* (6th ed.; D. Purves, G. J. Augustine, D. Fitzpatrick, W. C. Hall, A.-S. LaManita, R. D. Mooney, … L. E. White, Eds.). Sunderland, Massachusetts: Oxford University Press.

Russell, G., & Lightman, S. (2019). The human stress response. *Nature Reviews Endocrinology*, *15*(9), 525–534. https://doi.org/10.1038/s41574-019-0228-0

Santhakumar, V. (2006). Contributions of the GABAA Receptor 6 Subunit to Phasic and Tonic Inhibition Revealed by a Naturally Occurring Polymorphism in the 6 Gene. *Journal of Neuroscience*, *26*(12), 3357–3364. https://doi.org/10.1523/JNEUROSCI.4799-05.2006

Saunders, J. B., Aasland, O. G., Babor, T. F., Fuente, J. R. D. E. L. A., Grant, M., & Saunders, J. B. (1993). Development of the Alcohol Use Disorders Identification Test (AUDIT). *Addiction*, 791–804.

Schwabe, L., Haddad, L., & Schächinger, H. (2008). HPA axis activation by a socially evaluated cold-pressor test. *Psychoneuroendocrinology*, *33*(6), 890–895. https://doi.org/10.1016/j.psyneuen.2008.03.001

Schwabe, L., & Schächinger, H. (2018). Ten years of research with the Socially Evaluated Cold Pressor Test: Data from the past and guidelines for the future. *Psychoneuroendocrinology*, *92*(March), 155–161. https://doi.org/10.1016/j.psyneuen.2018.03.010

Segerstrom, S. C., & Miller, G. E. (2004). Psychological stress and the human immune system: A meta-analytic study of 30 years of inquiry. *Psychological Bulletin*, *130*(4), 601–630. https://doi.org/10.1037/0033-2909.130.4.601

Shaham, Y., & Stewart, J. (1995). Stress reinstates heroin-seeking in drug-free animals: An effect mimicking heroin, not withdrawal. *Psychopharmacology*, *119*(3), 334–341. https://doi.org/10.1007/BF02246300

Sharp, B. M. (2017). Basolateral amygdala and stress-induced hyperexcitability affect motivated behaviors and addiction. *Translational Psychiatry*, *7*(8), e1194–e1194. https://doi.org/10.1038/tp.2017.161

Sinha, R., Lacadie, C., Skudlarski, P., & Wexler, B. E. (2004). Neural Circuits Underlying Emotional Distress in Humans. *Annals of the New York Academy of Sciences*, *1032*(1), 254–257. https://doi.org/10.1196/annals.1314.032

Sklerov, M., Dayan, E., & Browner, N. (2019). Functional neuroimaging of the central autonomic network: recent developments and clinical implications. *Clinical Autonomic Research*, *29*(6), 555–566. https://doi.org/10.1007/s10286-018-0577-0

Spencer, Robert L & Deak, T. (2017). A User's Guide to HPA Axis Research. *Physiology & Behavior*, *176*(5), 139–148. https://doi.org/10.1016/j.physbeh.2017.03.040

Stagg, C. J., Bachtiar, V., & Johansen-Berg, H. (2011). What are we measuring with GABA Magnetic Resonance Spectroscopy? *Communicative & Integrative Biology*, *4*(5), 573–575. https://doi.org/10.4161/cib.16213

Steptoe, A., & Kivimäki, M. (2012). Stress and cardiovascular disease. *Nature Reviews Cardiology*, *33*(9), 360–370. https://doi.org/10.1038/nrcardio.2012.45

Sterling, P., & Eyer, P. (1988). Allostasis: a new paradigm to explain arousal pathology. In Handbook of Life Stress, Cognition and Health. *Handbook of Life Stress, Cognition and Health*, (September), 629–649.

Taggart, P., Critchley, H., van Duijvendoden, S., & Lambiase, P. D. (2016). Significance of neuro-cardiac control mechanisms governed by higher regions of the brain. *Autonomic Neuroscience: Basic and Clinical*, *199*, 54–65. https://doi.org/10.1016/j.autneu.2016.08.013

Tank, A. W., & Wong, D. L. (2015). Peripheral and central effects of circulating catecholamines. *Comprehensive Physiology*, *5*(1), 1–15. https://doi.org/10.1002/cphy.c140007

Task Force of the European Society Electrophysiology. (1996). Heart Rate Variability: Standards of Measurement, Physiological Interpretation, and Clinical Use. *Circulation*, *93*(5), 1043–1065. https://doi.org/10.1161/01.CIR.93.5.1043

Terpstra, M., Cheong, I., Lyu, T., Deelchand, D. K., Emir, U. E., Bednařík, P., … Öz, G. (2016). Test-retest reproducibility of neurochemical profiles with short-echo, single-voxel MR spectroscopy at 3T and 7T. *Magnetic Resonance in Medicine*, *76*(4), 1083–1091. https://doi.org/10.1002/mrm.26022

Tukey, J. W. (1977). Exploratory Data Analysis. *Biometrical Journal*, 866.

Ulrich-Lai, Y. M., & Herman, J. P. (2009). Neural regulation of endocrine and autonomic stress responses. *Nature Reviews. Neuroscience*, *10*(6), 397–409. https://doi.org/10.1038/nrn2647

Van Ast, V. A., Cornelisse, S., Meeter, M., Joëls, M., & Kindt, M. (2013). Time-dependent effects of cortisol on the contextualization of emotional memories. *Biological Psychiatry*, *74*(11), 809–816. https://doi.org/10.1016/j.biopsych.2013.06.022

van Marle, H. J. F., Hermans, E. J., Qin, S., & Fernández, G. (2009). From Specificity to Sensitivity: How Acute Stress Affects Amygdala Processing of Biologically Salient Stimuli. *Biological Psychiatry*, *66*(7), 649–655. https://doi.org/10.1016/j.biopsych.2009.05.014

van Marle, H. J. F., Hermans, E. J., Qin, S., & Fernández, G. (2010). Enhanced resting-state connectivity of amygdala in the immediate aftermath of acute psychological stress. *NeuroImage*, *53*(1), 348–354. https://doi.org/https://doi.org/10.1016/j.neuroimage.2010.05.070

van Oort, J., Tendolkar, I., Hermans, E. J., Mulders, P. C., Beckmann, C. F., Schene, A. H., … van Eijndhoven, P. F. (2017). How the brain connects in response to acute stress: A review at the human brain systems level. *Neuroscience & Biobehavioral Reviews*, *83*, 281–297. https://doi.org/10.1016/J.NEUBIOREV.2017.10.015

Varese, F., Smeets, F., Drukker, M., Lieverse, R., Lataster, T., Viechtbauer, W., … Bentall, R. P. (2012). Childhood adversities increase the risk of psychosis: A meta-analysis of patient-control, prospective-and cross-sectional cohort studies. *Schizophrenia Bulletin*, *38*(4), 661–671. https://doi.org/10.1093/schbul/sbs050

Watson, D., Clark, L. A., & Tellegen, A. (1988). Development and Validation of Brief Measures of Positive and Negative Affect: The PANAS Scales. *Journal of Personality and Social Psychology*, *54*(6), 1063–1070. https://doi.org/10.1037/0022-3514.54.6.1063

Yoon, B. E., Jo, S., Woo, J., Lee, J. H., Kim, T., Kim, D., & Lee, C. J. (2011). The amount of astrocytic GABA positively correlates with the degree of tonic inhibition in hippocampal CA1 and cerebellum. *Molecular Brain*, *4*(1), 1–7. https://doi.org/10.1186/1756-6606-4-42